Sole copy
Return to Chen

Oscillations and Diffusion in a Shear Stabilized Q-Machine

by

Francis F. Chen

MATT-522 February 15, 1967

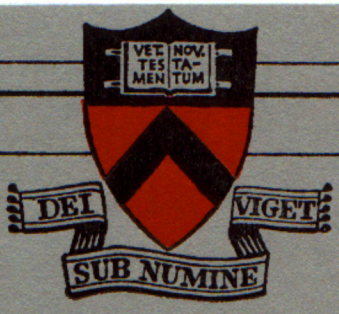

PLASMA PHYSICS LABORATORY

Contract AT(30-1)—1238 with the
US Atomic Energy Commission

PRINCETON UNIVERSITY
PRINCETON, NEW JERSEY

Princeton University
Plasma Physics Laboratory
Princeton, New Jersey

Oscillations and Diffusion in a Shear Stabilized Q-Machine

by

Francis F. Chen

MATT-522 February 15, 1967

Paper presented at the International Conference on Physics of Quiescent Plasmas, Frascati, Italy, January 1967.

AEC RESEARCH AND DEVELOPMENT REPORT

This work was supported under Contract AT(30-1)-1238 with the Atomic Energy Commission.

Oscillations and Diffusion in a Shear Stabilized Q-Machine

by

Francis F. Chen
Plasma Physics Laboratory, Princeton University, Princeton, New Jersey

I. INTRODUCTION

Recent theoretical work has indicated the importance to plasma stability and confinement of universal collisionless instabilities /1/, resistive drift modes /2/, collisionless quasimodes /3-4/, and resistive quasimodes /4/. The purpose of this experiment is to investigate these instabilities in a thermally ionized potassium plasma, and particularly the effect of magnetic shear on these waves and on diffusion.

It has been shown /2/ that thermionic plasmas are also subject to flute instabilities with $k_{||} = 0$ excited by the centrifugal force due to plasma rotation. To eliminate these, we operate with two hot endplates with electron sheaths; the theory of line-tying in Q-machines /5/ then shows that only modes with finite $k_{||}$ can exist. Under such conditions the conducting endplates dominate the behavior of the plasma, and the plasma is quite stable unless it is sufficiently long. By creating a plasma 325 cm long, we have approximated the conditions in a fusion device, such as a stellarator, which has a long region of unfavorable magnetic curvature between regions of good curvature, where the perturbations are line-tied. Furthermore, with radius R = 2.5 cm and field B_z = 4 kG, the ratio r_L/R = .04 is small, as in fusion devices.

We have covered peak densities from 10^9 cm^{-3}, where the ion-electron mean free path λ_{ei} is 100 cm, to 3×10^{11}, where λ_{ei} = 3 mm. Previous experiments at low densities /6/ were performed in a plasma so short (L ≈ 30 cm) that it is not clear how resonant electrons can have time to excite a collisionless universal instability before colliding with an endplate. With L = 325 cm, this process is still difficult, but much more plausible.

In the absence of longitudinal currents, two other instabilities are possible in this plasma: the well-known temperature-gradient universal instability and the Kelvin-Helmholtz instability /7/. We have tried to avoid these, at least in the interior of the plasma, by making the endplates closely isothermal at the same temperature, and by equalizing the input flux of neutral atoms at the ends of the machine to minimize macroscopic drifts.

II. APPARATUS

Figure 1 is a schematic of the coaxial hot plate and collimator assembly used at each end of the machine. The hot plate is a tungsten disk 6.4 cm in dia. and 1.3 cm thick, with a 1.3 cm dia. central hole. The plate is heated by electron bombardment at 2 kV from a series-parallel arrangement of curved tungsten filaments 0.5 mm in dia. A grounded Mo tube extending nearly up to the hot plate prevents high-energy electrons from entering the plasma through the axial access hole. All ceramic insulators are of boron nitride, are in the shape of rings, and are cooled by conduction to the copper housing for the hot plate assembly. The latter fits snugly into the 15-cm dia. externally water-cooled copper vacuum chamber; no internal water-cooling is necessary. With 6 kW of bombardment power, the hot plates reach 2600°K. Uniformity of

temperature is achieved by using thick plates, by careful alignment of the filaments with the plate, and by masking of the edge of the plate by a 5.1-cm dia. Mo aperture limiter. The temperature is normally uniform to $\pm$ 6°K.

The neutral beam is collimated by two annular slits (Fig. 1); in addition, a cooled Cu "scraper" greatly reduces the neutral flux near the edge of the hot plate. The stainless steel collimator is heated to 400°C by radiation from the endplate and is divided into two compartments. In the compartment with the slits, the neutral pressure is always so low that the mean free path λ is longer than the dimensions ℓ of the chamber. Thus the shape of the beam is independent of the neutral flux. In the rear compartment, connected to the front compartment by 12 small holes, the pressure is always so high that $\lambda << \ell$; thus the neutrals are evenly distributed azimuthally. The neutral atoms are piped into the rear chamber from an external oven via a hot Cu tube. Vacuum-distilled potassium is used.

Figure 2 shows a schematic of the machine. The magnetic field coils provide up to 4 kG dc with 1% uniformity. The base pressure is about 5×10^{-6} torr. The neutral K pressure is negligible because the vacuum chamber is water-cooled. The shear field is provided by a water-cooled Al tube 1-cm in dia. strung thru the 1.3-cm dia. holes in the hot plates. The holes are previously aligned along B_z by an electron beam. The axial conductor is supported at points 600 cm apart and is kept taut by a lever arrangement providing 1/2 ton of tension. The deflection due to gravity is less than 0.2 mm. The maximum dc current I_s in the axial conductor is 5 kA. A view

of one end of the machine is shown in Fig. 3.

The neutral flux distribution is measured by inserting two hinged collectors (cold plates), thus coverting the double-ended machine into two single-ended ones of ordinary length. If a large negative bias is applied to the collector and an electron sheath is created at the hot plate, all ions created there flow unidirectionally to the collector, and a probe can measure their distribution. The ion current collected by the cold plate is a measure of the input flux. All plasma properties are measured by small Langmuir probes 0.25 or 0.05 mm in dia. by 2mm long; these are described in another paper /8/. Radial scans are made in 30 sec by automatic probe drives. Frequency analysis is made by a Panoramic Model SPA-3/25a Spectrum Analyzer or (below 5 kHz) by a Panoramic Model SB-15a ultrasonic Spectrum Analyzer; both are driven by a Tektronix Model 1A7 preamplifier.

III. CLASSIFICATION OF OSCILLATIONS

Fluctuations in ion and electron saturation currents to the probes and in floating potential of the probes do not, in general, have a repetitive waveform but have a continuous frequency spectrum. These fluctuations fall into three categories, which we define as follows: 1) low-frequency (*l.f.*) oscillations extending up to about 5 kHz; 2) medium-frequency (m.f.) oscillations roughly between 5 and 50 kHz; and 3) high-frequency (h.f.) oscillations from 50 kHz to beyond 500 kHz, which is the upper limit of our frequency response. Examples of the spectra in these three regions are shown in Fig. 4.

In the absence of shear, the plasma appears to be completely turbulent,

with $\tilde{n}/<n>$ of order unity, where $\tilde{n}$ is the peak to peak fluctuation in density. We believe that the absence of a quiescent plasma and discrete oscillations, as found in other Q-machines, is caused by the great length of the plasma, which allows instabilities with very small $k_{\parallel}$ to grow to large amplitudes in spite of the conducting endplates. For example, if the machine is operated single-ended (only one hot plate), we can change from L = 325 cm to L = 70 cm by inserting a collector plate; the l.f. fluctuation amplitude then decreases a factor of 10, and the h.f. by a factor of 2. Thus one method of approaching quiescence is to decrease L.

A second method is to decrease the magnetic field B. The variation of fluctuation amplitude with B is shown in Fig. 5. Below a critical field B_c, the plasma is relatively quiescent, with $\tilde{n}/<n>$ of the order of a few percent. Only m.f. and h.f. noise appears below B_c. At B_c the l.f. oscillations abruptly set in, and $\tilde{n}/<n>$ reaches the order of unity at high fields. B_c is apparently the threshold for resistive drift waves, such as those observed by Hendel /9/; but the spectrum becomes continuous just beyond B_c and stays continuous even in the minimum near 2800 G (Fig. 5).

1) The high-frequency spectrum. In the range 50-500 kHz the spectrum is generally that of white noise, with a broad peak in the neighborhood of, but not exactly at, the ion cyclotron frequency. This peak, however, is not always present; and we have not identified it. The h.f. noise is larger at the edge of the plasma [$\tilde{n}/<n> = 0(1)$] than in the interior [$\tilde{n}/<n> = 0(2\%)$]. It is larger for $B < B_c$ than for $B > B_c$. It is smaller at the midplane of the

plasma than near the ends or in single-ended operation. It is insensitive to sheath conditions. In general, the presence of l.f. drift waves diminishes the h.f. noise.

The amplitude of the white noise is at least two orders of magnitude above what would be expected from thermal fluctuations. For instance, the mean square current fluctuation in a resistor R is given by

$$\langle \tilde{J}^2 \rangle = 4\,kT\Delta f/R, \qquad (1)$$

where Δf is the bandwidth of the detector. If we substitute for R the minimum value obtainable from a probe characteristic, namely, $R \approx kT/eJ_-$, the thermal value of $\langle \tilde{J}_-^2 \rangle / \langle J_- \rangle^2$ is $4e\Delta f/\langle J_- \rangle$. For $\langle J_- \rangle \approx 5 \times 10^{-6}$ A, $J_{-rms}/\langle J_- \rangle$ works out to be of the order of 2×10^{-4} or less for thermal fluctuations, whereas we observe $\approx 2 \times 10^{-2}$. The h.f. noise thus appears to be superthermal and may be the result of a h.f. instability such as the drift-cyclotron instability /10/. Note that we use J_- here because V_f has insufficient frequency response and J_+ is more sensitive to displacement current /8/.

None of the oscillations reported here is caused by fast electrons from the hot plate heater, because the spectra do not change when the bombardment voltage is suddenly removed.

2) The medium-frequency spectrum. The spectrum between 5 and 50 kHz is marked by the frequent appearance of a large peak between 10 and 20 kHz. At the low end, the m.f. spectrum joins onto the tail of the l.f. spectrum of drift waves, if any. Occassionally, the m.f. peak is accompanied by harmonics

at about 1 1/2 and 2 times the fundamental frequency f_o. The width of the peak varies, and the phenomenon is not exactly reproducible; the following observations are not always true.

The m.f. peak occurs with both single-ended and double-ended operation, regardless of the presence of resistive drift waves. The amplitude is largest at the edge of the plasma and vanishes 8mm from the edge (toward the axis), even if the density gradient is large there. f_o is generally independent of r. It also does not depend on probe potential. The spectrum is independent of axial position z. f_o increases with B, but not in a simple fashion; the peak disappears below 1.5 kG. f_o is independent of kT, but the peak disappears at low plate temperatures; the sheath is still electron rich at the critical temperature. When operating single-ended, the m.f. spectrum depends sensitively on the bias on the collector plate. When the hot plates are allowed to float relative to the aperture limiter, the m.f. peak disappears.

This oscillation appears very similar to one reported by Buchel'nikova et al. /6/. The frequency fits well with that of the collisionless universal instability with $kr_L \approx 1$ /11/; however, the above observations indicate that this phenomenon is associated with conditions at the plasma edge. Although f_o is higher than observed in the Kelvin-Helmholtz instability /7/ or the magnetoionic sound wave /12/, we cannot yet exclude these possibilities. A large electric field exists at the edge when the cathodes are grounded and the sheath is negative. We have indications that this causes a rise in kT_e at the edge, making a temperature-gradient instability possible.

3) The low-frequency spectrum. The large-amplitude low-frequency spectrum appearing above B_c (Fig. 5) is comparatively well understood. Away from the boundaries there are no currents, streams, anisotropies, or large electric fields to excite instabilities, and the oscillations are almost surely caused by the resistive drift instabilities driven by the pressure gradient and the centrifugal force /2/. It is now known /13/ that the radial electric field in a thermionic plasma ideally brings the electron diamagnetic drift velocity v_{De} down to zero in the laboratory frame; hence the drift waves do not propagate, and the spectrum is due to the non-linear growth of the waves. Actually, the waves have a finite real frequency because a) the radial electric field differs from the ideal one because of charge separation due to ion-ion and ion-neutral collisions and because of a finite temperature gradient in the hot plates (the latter gives a fundamental drift frequency of 10 Hz at best and 150 Hz at worst); and b) drift waves have $|\omega/k_\perp| < v_{De}$ if $k_\parallel$ is very small or if $k_\perp^2 r_L^2 = O(1)$.

These considerations explain why the observed *l.f.* spectrum (Fig. 4) is continuous and is peaked at a very low frequency. In homogeneous turbulence the $k_\perp$ spectrum should fall as $k_\perp^{-5}$ /14/ for $k_\perp R >> 1$, where R is a characteristic dimension of the plasma. The observed ω spectrum falls roughly as ω^{-3}; this is consistent with the k^{-5} spectrum, since $\omega/k_\perp$ is not constant for large $k_\perp$.

As expected with electron sheaths /5/, flute instabilities with $k_\parallel = 0$ driven by the centrifugal force are not observed; these would appear as a peak at the ion drift frequency ($\approx$ 700 Hz) for m = 1 /15/. The collisionless universal

instability /11/ is excluded because the l.f. oscillations disappear at low B fields such that $r_L/\Lambda \simeq 0$ (1), where Λ is the density scale length. This stabilization is apparently caused by viscous damping /9/ and would not occur for the collisionless instability.

The amplitude of the l.f. oscillations increases with density and plasma length and decreases with hot plate temperature, in agreement with the theory of end plate stabilization /5/. The radial dependence will be shown in Fig. 11. The amplitude peaks on the interior slope of the density profile (near the central hole) where the density gradient is steepest, but the plasma is so turbulent that the l.f. spectrum is seen everywhere inside the plasma. With a small amount of shear stabilization, the peak is moved to the normal position on the density gradient at the exterior of the plasma.

The incoherence of the l.f. fluctuations makes phase and velocity measurements difficult. However, the turbulence resembles that found in closed fusion devices; and this long Q-machine is ideal for studying diffusion due to drift waves because anomalous losses dominate over classical losses.

IV. SHEAR STABILIZATION

The effect on the frequency spectrum of a current I_s in the axial conductor providing a shear field is shown in Fig. 6 for the l.f. range and in Fig. 7 for the m.f. range. Only data at one value of B, one value of n, and one probe position are shown; but the data typically show that the l.f. oscillations are reduced by large shear ($I_s > 1$ kA).but the m.f. oscillations are not reduced as much. The effect of shear on the plasma density is shown in Fig. 7; the density is seen to increase a factor of 8 as I_s increases from 0 to 4 kA. At small I_s

(~ 250-500 A) the density is increased although the oscillation amplitude (Figs. 6 and 7) is not reduced. We attribute this to the fact that drift waves are localized even when not suppressed by shear, as predicted by theory /2/; and this localization reduces the diffusion coefficient $D_\perp$.

The plasma density is almost entirely controlled by diffusion, and hence the peak density is a measure of $D_\perp$. This is true because a) the density profiles do not resemble the flux distribution from the endplates but rather look like those predicted by diffusion theory; b) the equilibrium density computed from endplate recombination alone is much higher than that observed; and c) the density depends on B, as shown in Fig. 9. From data such as those of Fig. 9, we have computed an effective $D_\perp$ by neglecting the z-dependence of the density profile, which is small, and solving a simple radial diffusion equation with $n = 0$ at r_1 (the hole) and at r_2 (the aperture limiter). The resulting density distribution is

$$n(r) = \frac{\phi}{4D_\perp}\left[(r_2^2 - r_1^2)\frac{\ln(r/r_1)}{\ln(r_2/r_1)} - (r^2 - r_1^2)\right], \qquad (2)$$

which is not unlike the observed profiles. The derivative of this equation relates the peak density to $D_\perp$. The input flux ϕ is assumed to be independent of $\underline{r}$ and is measured as indicated in Sec. II. The absolute density is estimated from the probe current by using Langmuir's orbital theory for $r_p/\lambda_D < 3$ and Lam's theory for $r_p/\lambda_D > 3$ /16/.

In Fig. 10 are shown the results for the variation of $D_\perp$ with shear. We have taken out the B dependence by normalizing $D_\perp$ to the Bohm coefficient, computed neglecting B_θ, whose effect on $|B|$ is very small, and by plotting

against the shear parameter θ, defined by $\theta = | r\, \partial/\partial r\, (B_\theta/rB_z) | \Lambda$ and evaluated at r = 2 cm. The points for different values of B_z fall on the same line, showing that only the angle θ is relevant for shear stabilization. The absolute magnitude of $D_\perp/D_B$ is uncertain by a factor of 3 because of the use of probes for absolute density measurements in a magnetic field and because of the arbitrary constant used in D_B. However, the relative error in the points is less than 20%; it arises mainly from the deviation of the observed profiles from that of Eq. (2). The points at $I_s \geq 4$ kA have a somewhat larger error due to the following effect. The water-cooled axial conductor is usually coated with a layer of potassium atoms. When the rod is heated by I_s, this layer evaporates and increases the neutral flux to the hot plates, thus increasing the plasma density. This is seen as a slow rise in the collector current at the end where the cooling water exits. This effect has been corrected for, the correction amounting to about 16% at 4 kA. Another source of error is the electric field caused by the potential drop along the axial conductor. This field may cause instabilities or may stabilize them by velocity shear. Having found that positive potentials on the conductor have little effect on the oscillations, we grounded the negative end of the conductor. Subsequent experiments with an insulated conductor have confirmed the insensitivity of the diffusion measurements to such electric fields.

Localization of oscillations by shear is illustrated in Figs. 11-13, which are x-y recorder traces of mean square oscillation amplitude vs. radius in relation to the density profile. Also shown are dc-coupled oscillograms of the oscillations at various radii showing the perturbation level. At zero

shear (Fig. 11), the large broad peaks are due to l.f. oscillations; the small peaks near the edge are m.f. and h.f. oscillations. With I_s = 1 kA (Fig. 12), the oscillations are stabilized near the axis, where B_θ is large, and the drift wave peaks occur on the outer density gradient, as they should. Note that the amplitude of oscillation at the peaks, as seen on the oscillograms, is not greatly reduced. The h.f. peaks at the edge are larger than in Fig. 11. With I_s = 3kA (Fig. 13), the oscillation peaks are narrower, and several can be seen along the outer density gradient. The drift wave peaks C and E are now quite small, but the h.f. peak A is still large. Peaks B and F contain both h.f. and l.f. Note the local flattening of the density profile near the l.f. peaks. H.f. and m.f. oscillations at the edge of the plasma apparently cause less diffusion than the l.f. oscillations in the interior; however, the 1 kG curve of Fig. 9 clearly shows that there is anomalous transport for $B < B_c$, when no l.f. oscillations exist.

In conclusion, Fig. 10 has shown a decrease of an order of magnitude in $D_\perp$ when shear is applied to a plasma with low-frequency turbulence. However, no critical value of shear up to $\theta = 0.5$ stops all the oscillations; rather, there is a gradual improvement with increasing θ. The shear applied exceeds the theoretical stabilization criteria for collisionless normal modes /1/, collisionless quasimodes /3-4/, resistive normal modes /2/, and resistive quasimodes /4/. The decrease in $D_\perp$ has been shown to be associated with the localization of oscillations by shear. This experiment demonstrates for the first time the effectiveness of shear alone in stabilizing resistive instabilities.

We are indebted to D. Mosher for collaborating in all aspects of this work, to K. P. Mann and A. B. Chianese for operation of the machine, to W. Lamont for construction of probes and hot plate assemblies, to J. Joyce for design of the axial conductor, and to H. Hendel and S. von Goeler for stimulating discussions. This work was performed under the auspices of the U. S. Atomic Energy Commission, Contract No. AT(30-1)-1238.

REFERENCES

/1/: N. A. Krall and M. N. Rosenbluth, Phys. Fluids 8, 1488 (1965).

/2/: F. F. Chen, Phys. Fluids 9, 965 (1966).

/3/: P. Rutherford and E. A. Frieman, PPL MATT-476 (1967).

/4/: B. Coppi, G. Laval, R. Pellat, and M. N. Rosenbluth, Document IC/65/88, IAEA International Centre for Theoretical Physics, Trieste, 1965.

/5/: F. F. Chen, J. Nucl. Energy, Pt. C, 7, 399 (1965).

/6/: N. S. Buchel'nikova, A. M. Kudryavtsev, and R. A. Salimov, Zh. Tekhn. Fiz. 35, 72 (1965) [English transl.: Soviet Phys.-Tech. Phys. 10, 53 (1965)].

/7/: N. D'Angelo and S. von Goeler, Phys. Fluids 9, 309 (1966).

/8/: F. F. Chen, subsequent paper in the Proceedings of the International Conference on Physics of Quiescent Plasmas, Frascati, 1967.

/9/: H. Hendel and P. Politzer, subsequent paper in the Proceedings of the International Conference on Physics of Quiescent Plasmas, Frascati, 1967.

/10/: F. F. Chen, Phys. Fluids 7, 949 (1964).

/11/: B. B. Kadomtsev and A. V. Timofeev, Dokl. Akad. Nauk SSSR 146, 581 (1962) [English transl.: Soviet Phys.-Doklady 7, 826 (1963)].

/12/: M. Porkolab and G. S. Kino, Phys. Rev. Letters 15, 752 (1965).

/13/: F. F. Chen, PPL MATT-472 (1966), Phys. Fluids 10, (1967).

/14/: F. F. Chen, Phys. Rev. Letters 15, 381 (1965).

/15/: F. F. Chen, Paper 6R-15S presented at the Eighth Annual Meeting of the Division of Plasma Physics, American Physical Society, Boston, 1966 (to be published).

/16/: F. F. Chen, J. Nucl. Energy, Pt. C, 7, 47 (1965).

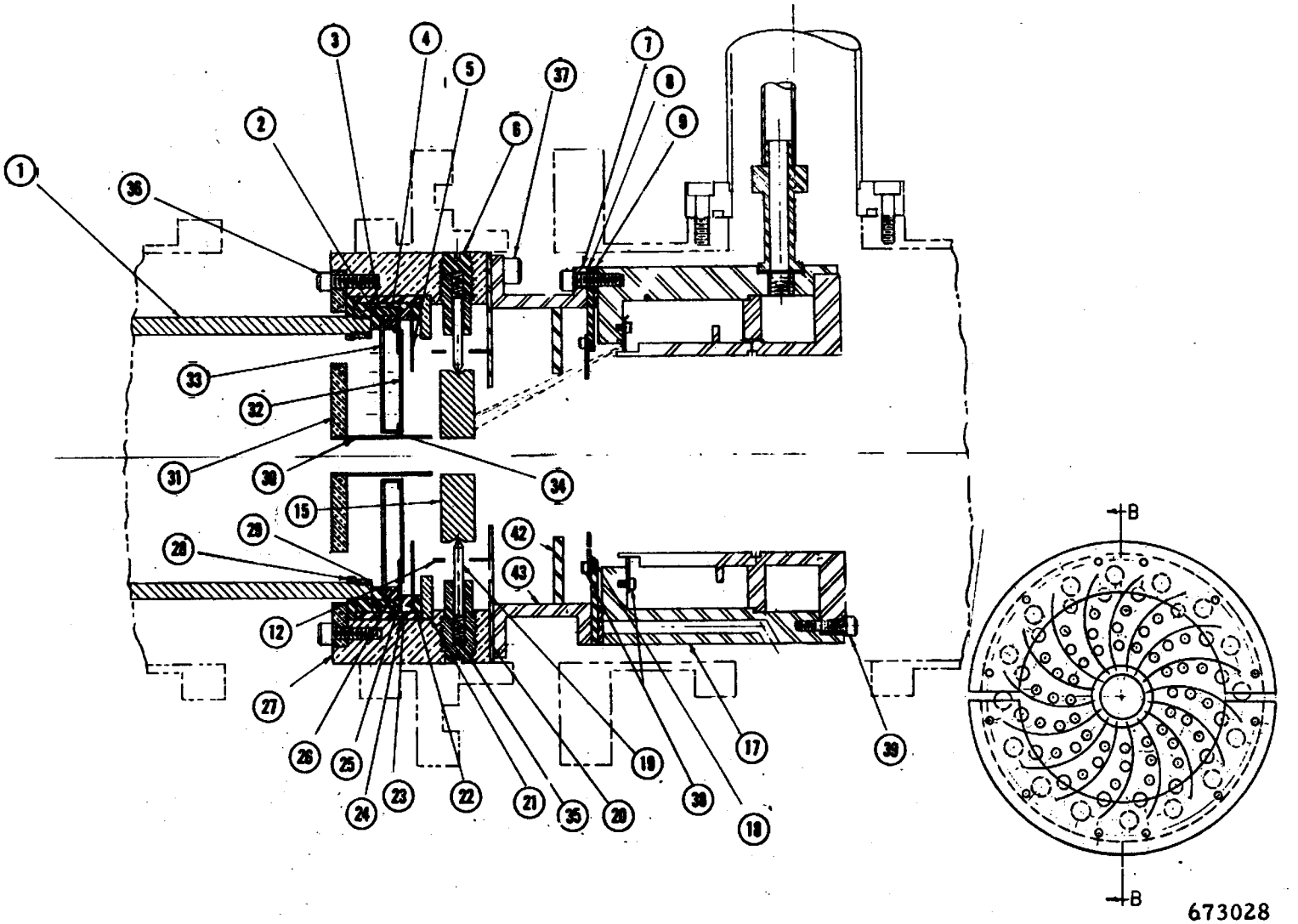

Fig. 1. Scale drawing of the hot plate and filament assembly and the neutral beam collimator. The inset shows a front view of the filaments; the holes in the shield behind them are for pumping.

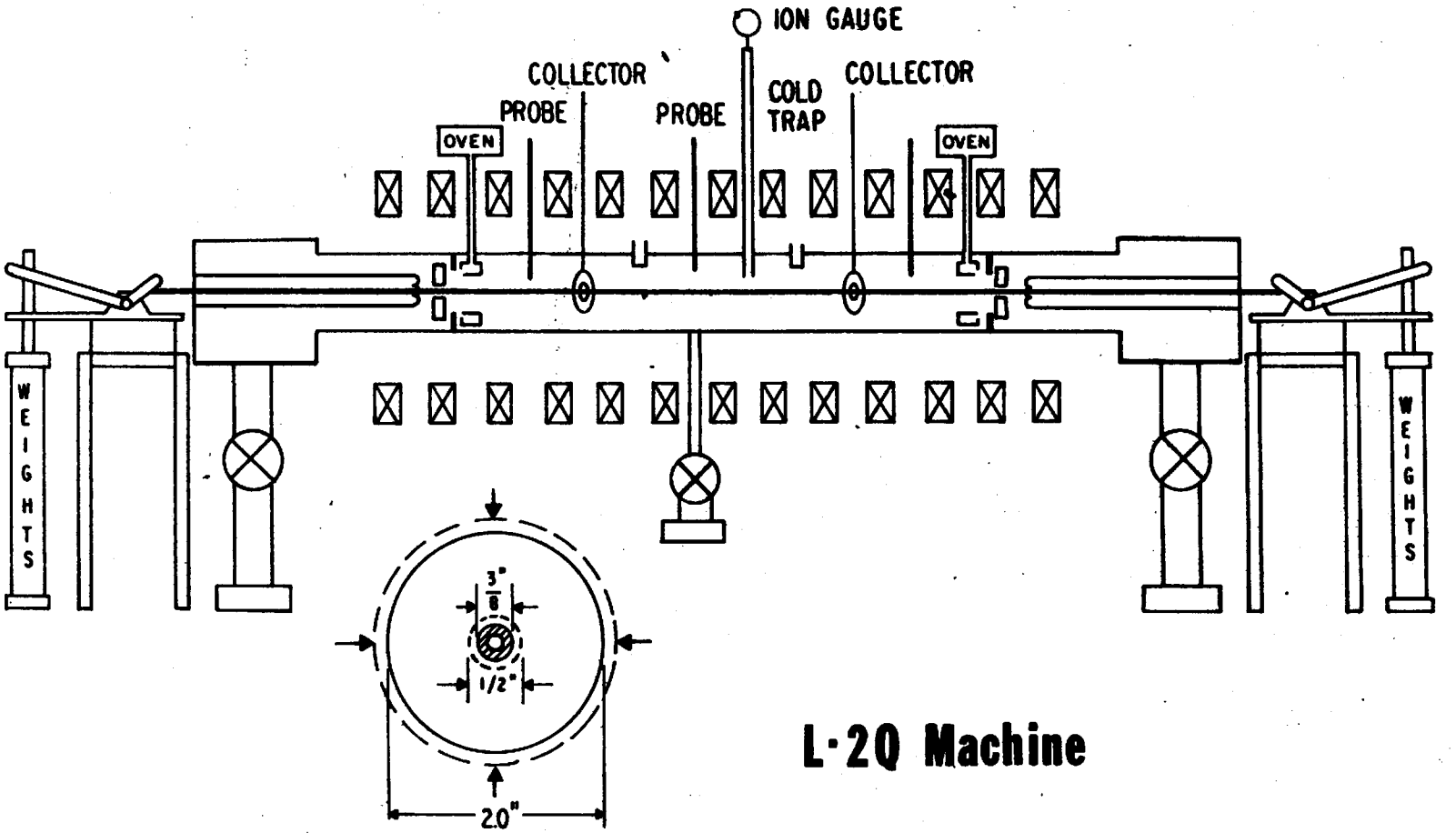

673025

Fig. 2. A simplified schematic (not to scale) of the L-2 Q machine showing the axial conductor passing through the coaxial end plate assemblies.

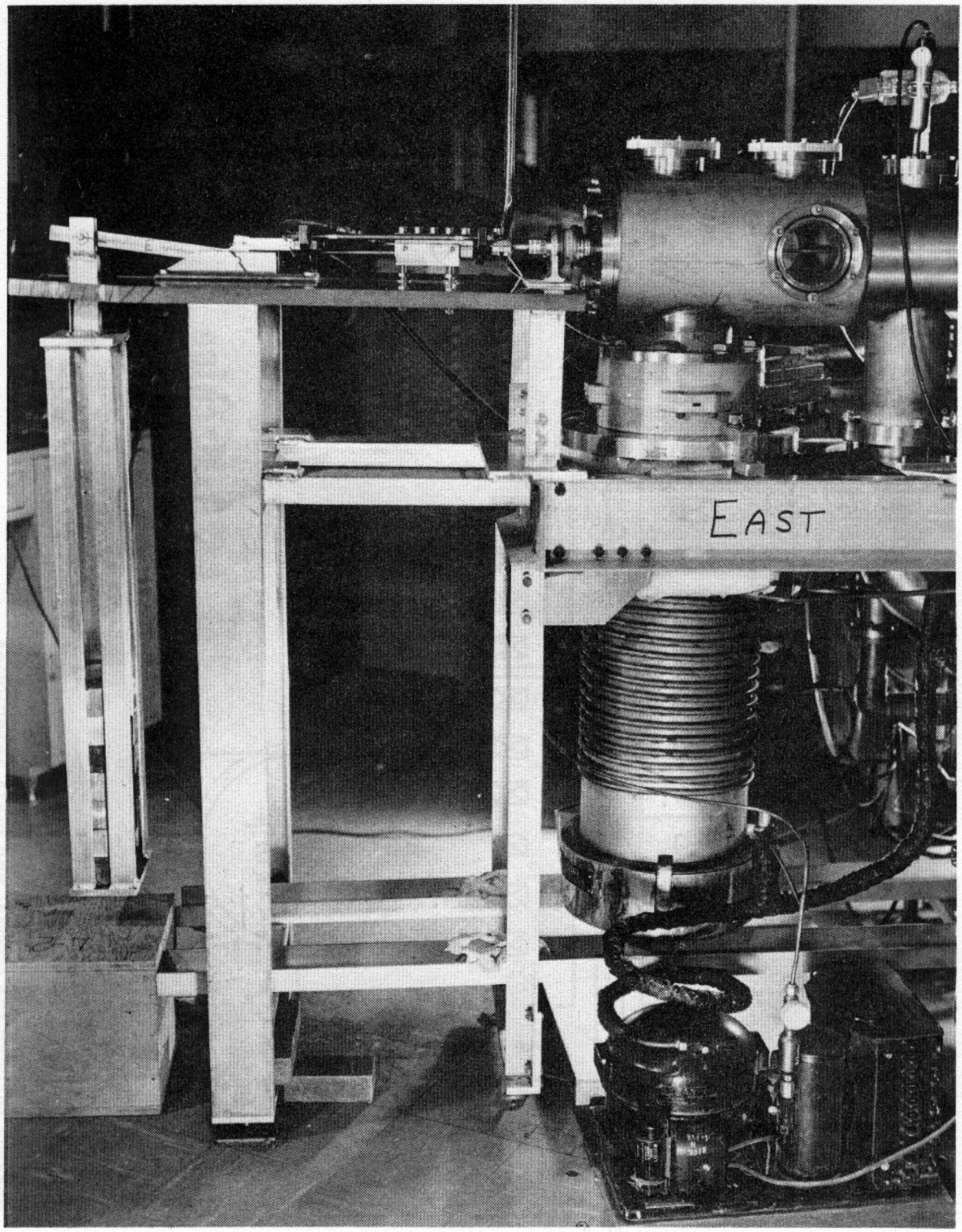

663201

Fig. 3. Photograph of one end of the L-2 A machine, showing the lead weights and lever arrangement for tensioning the axial conductor.

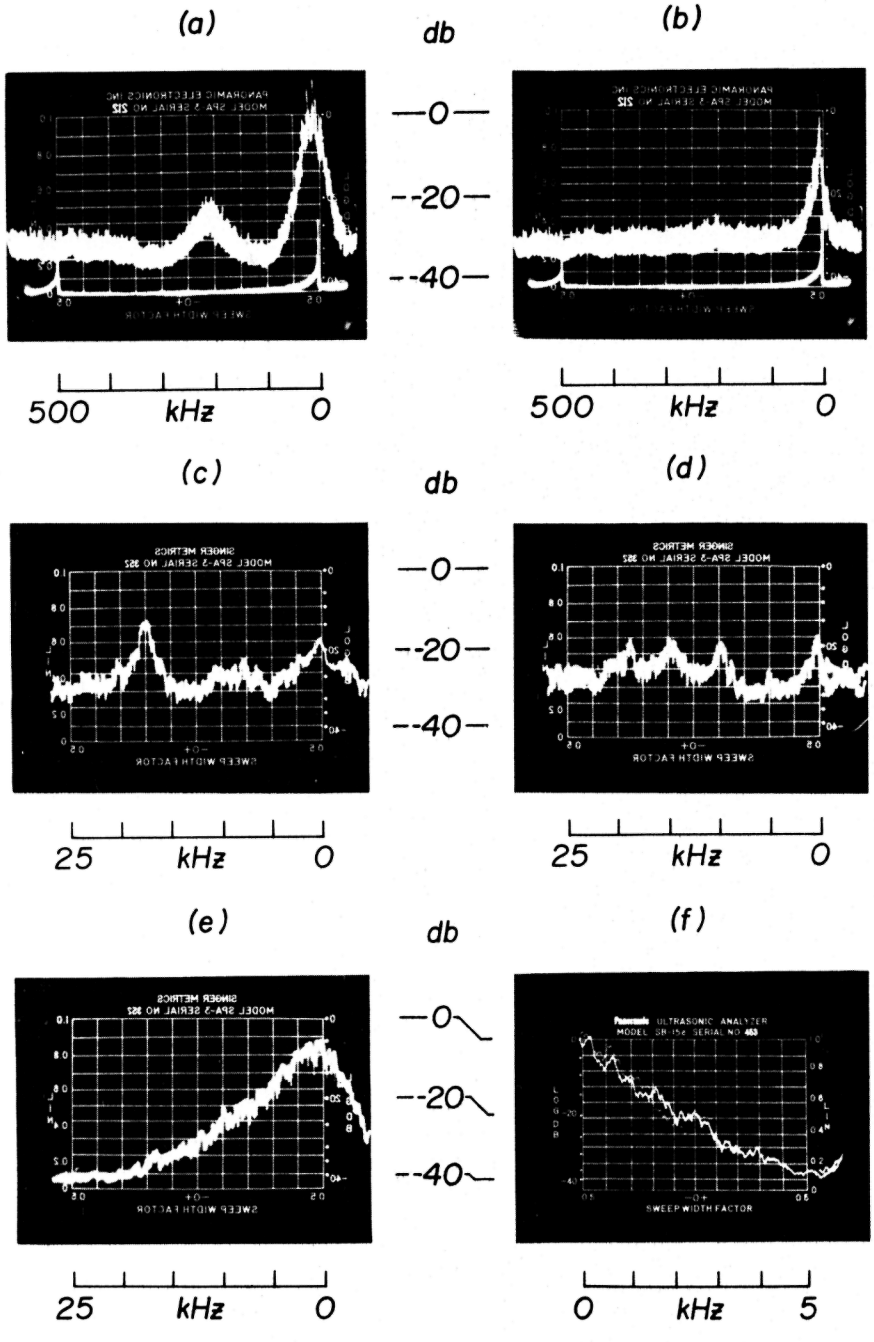

673035

Fig. 4. Examples of the spectra of the three types of oscillations. These may or may not occur simultaneously at a given radial position. They are found with all three probe detection methods (J_+, J_-, V_f), with or without the axial conductor or the hole in the end plates. (a) and (b) are h.f. spectra with and without the h.f. peak. (c), (d), and (e) are m.f. spectra with a single m.f. peak, with harmonics, and with no peak. (f) is the l.f. drift wave spectrum.

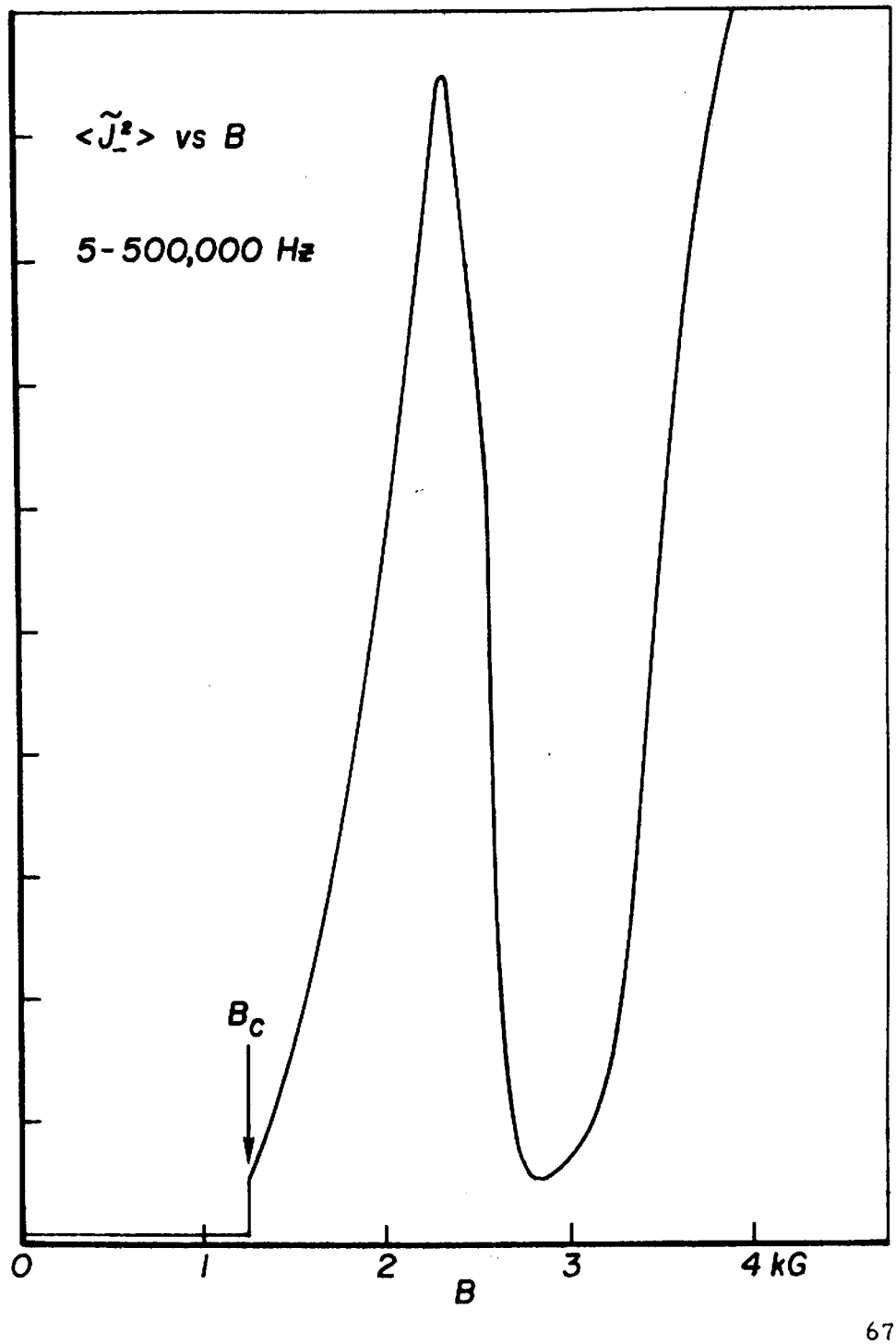

673027

Fig. 5. The mean square fluctuation amplitude in electron saturation current, in the band 5 Hz to 500 kHz, as a function of magnetic field, in the absence of shear, at a fixed probe position. The data were taken on an x-y recorder with a biased-diode squaring voltmeter.

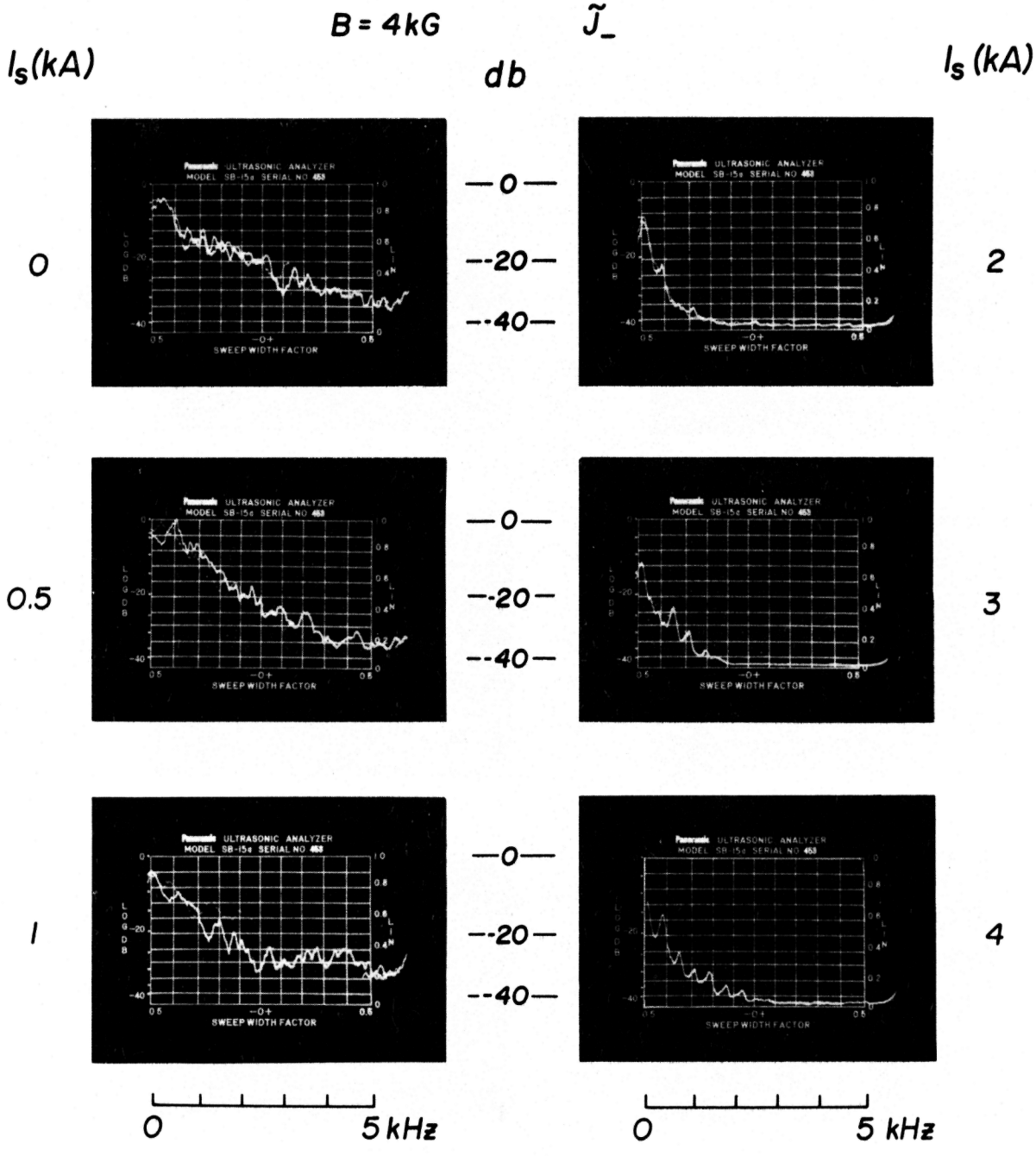

673032

Fig. 6. Effect of shear current I_s on the l.f. spectrum at low plasma density. The same gain is used throughout; the oscillation amplitude has not been normalized to the dc probe current.

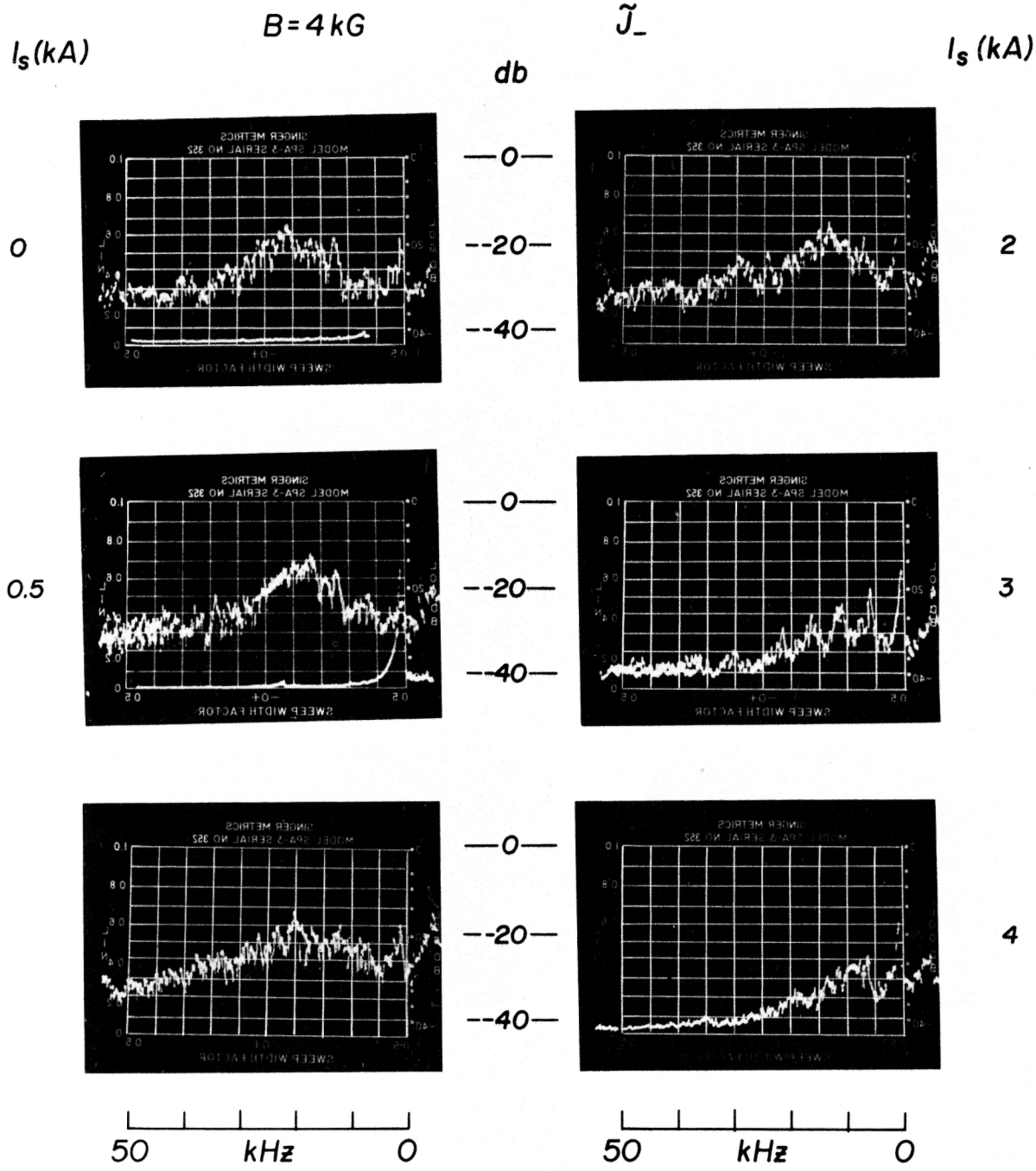

Fig. 7. Effect of shear current I_s on the m.f. spectrum at low density. The lower traces indicate the noise level of the circuitry.

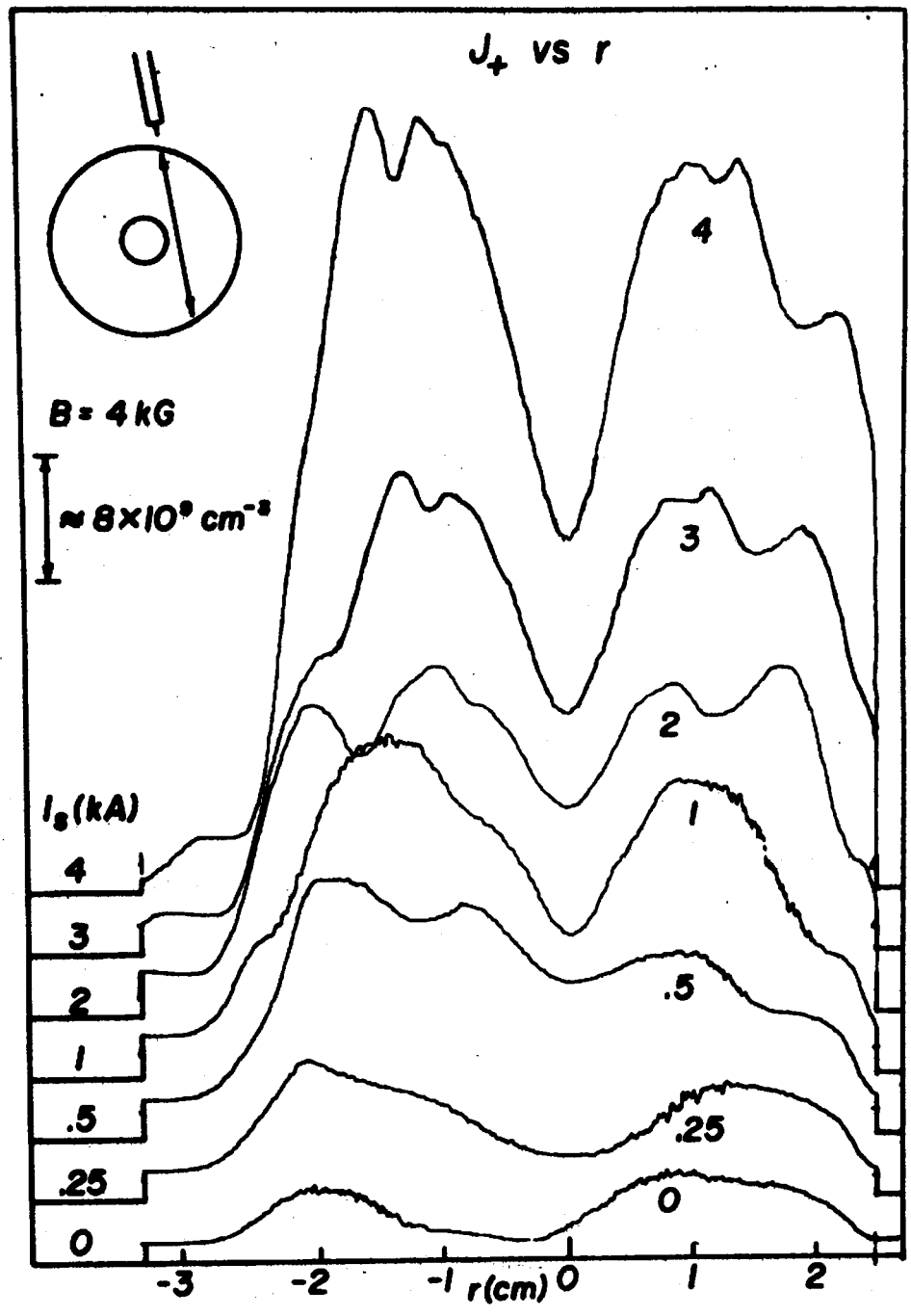

673033

Fig. 8. X-y recorder traces of ion saturation probe current versus radius for various values of shear current I_s. Note that the baseline has been shifted for successive curves. The probe was moved off axis to just miss the axial conductor.

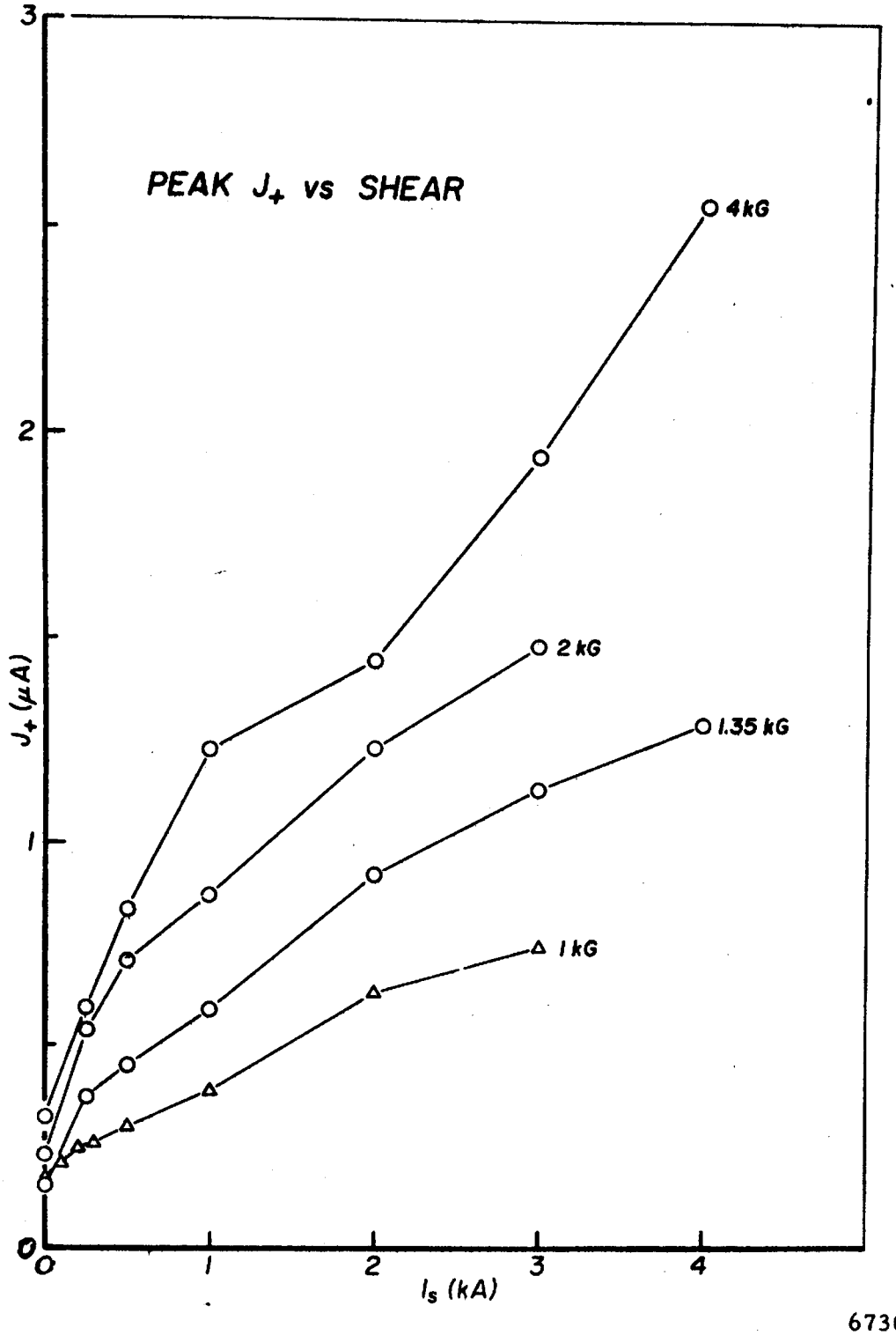

Fig. 9. Variation of peak density (probe current) with shear, for various values of B_z.

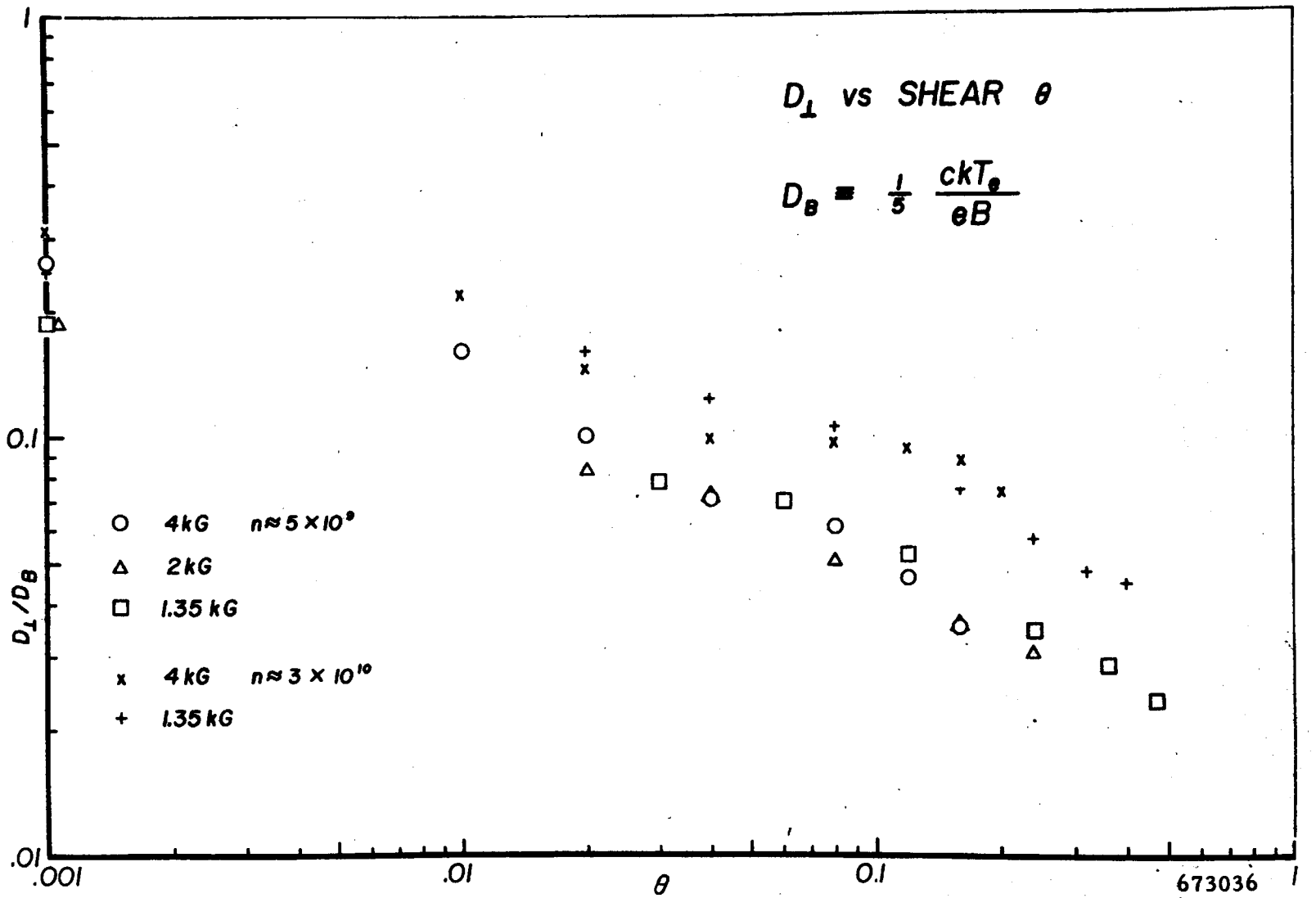

Fig. 10. Decrease of effective diffusion coefficient with shear, at two densities. The points at $\theta = 0.001$ are those taken at $I_s = 0$. Classical losses are estimated to lie below the bottom of the graph in all cases.

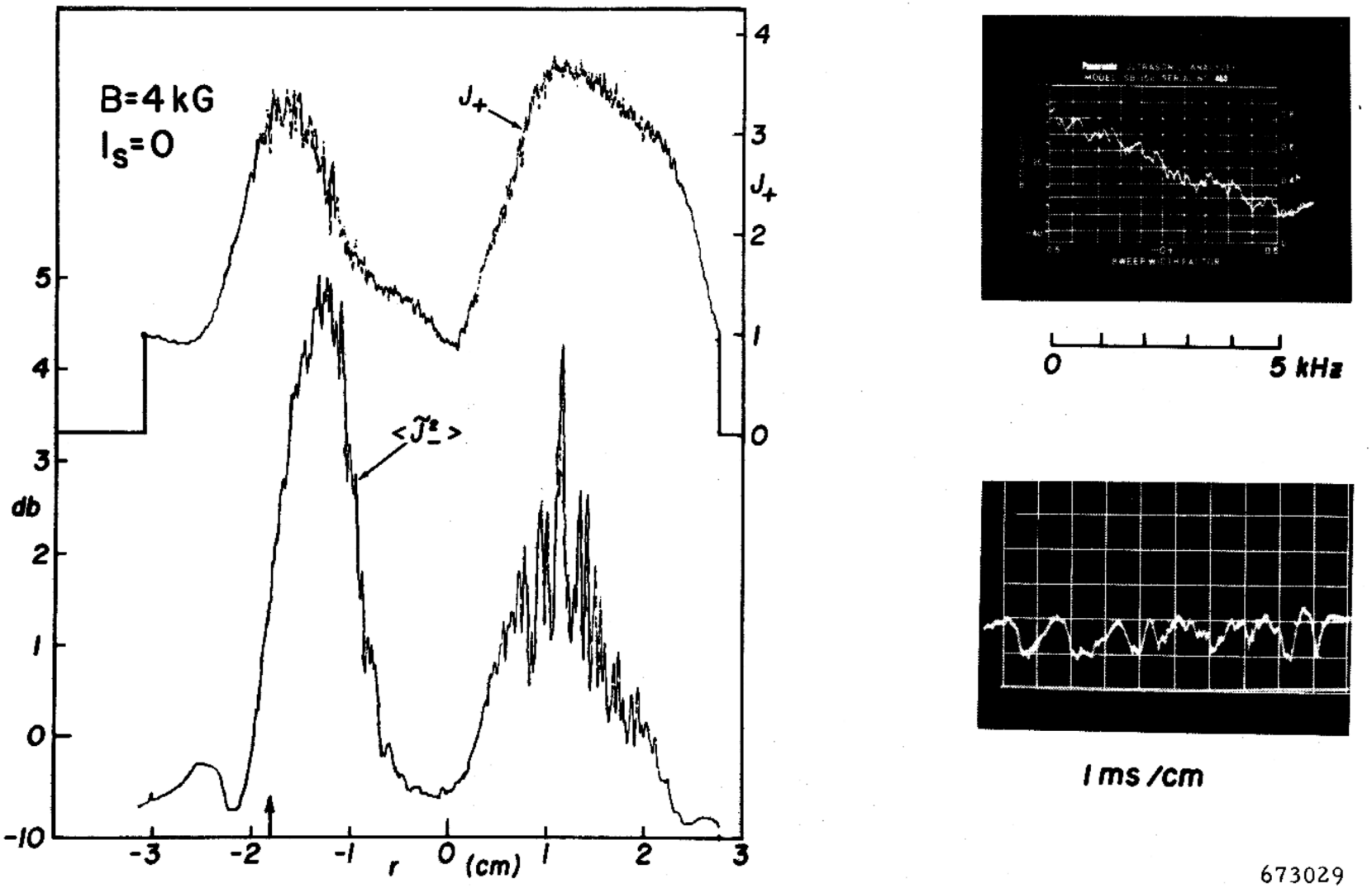

Fig. 11. The density profile and mean square oscillation profile, in the range 5 Hz - 500 kHz (arbitrary units) for $I_s = 0$. Note that the oscillation amplitude has not been normalized to the density. For the radius indicated by the arrow, the frequency spectrum and probe trace are shown. The dc level of the probe current is shown by the distance to the zero trace at the bottom.

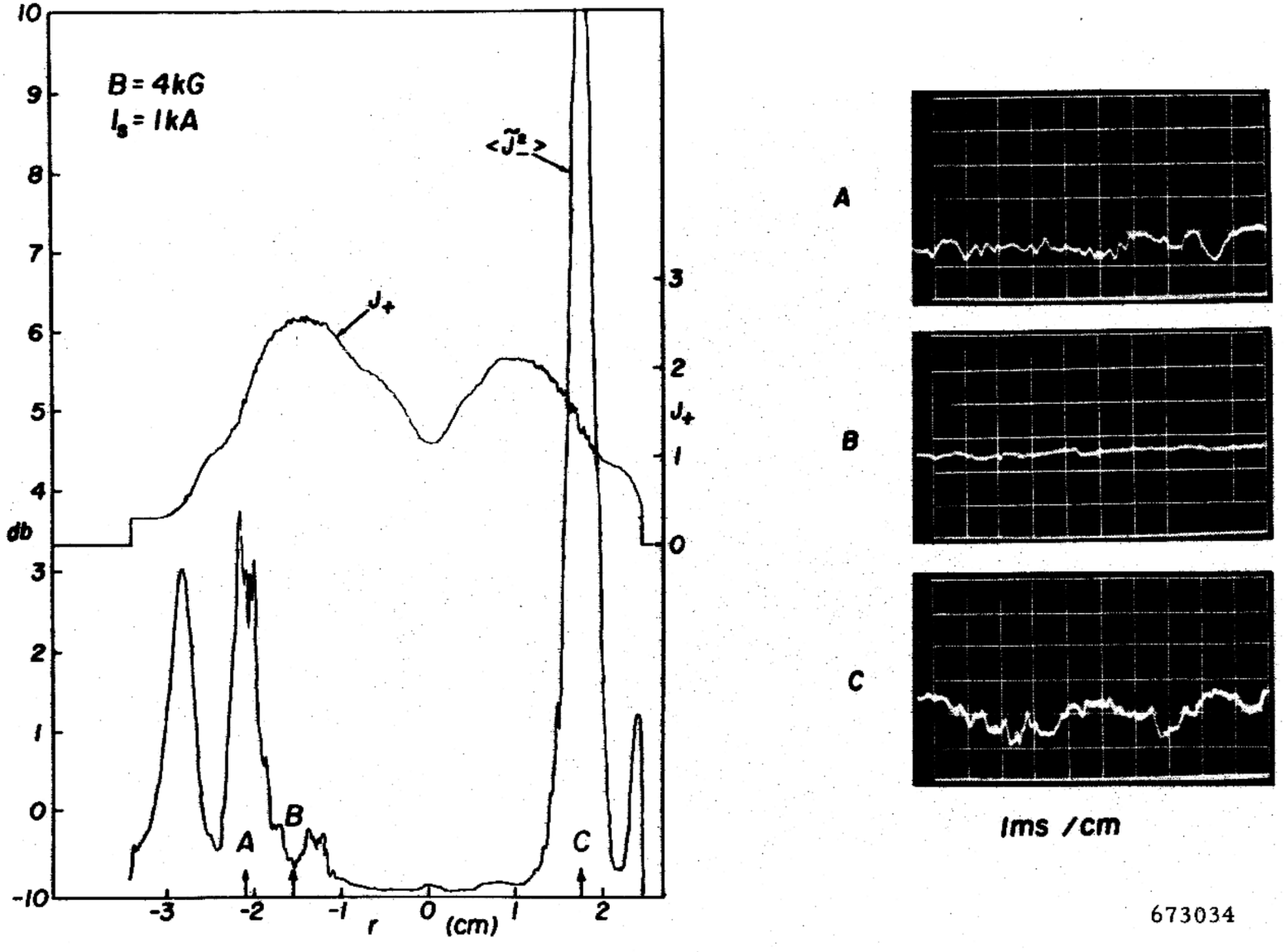

Fig. 12. Density and oscillation profiles at I_s = 1 kA. Other comments of Fig. 11 apply.

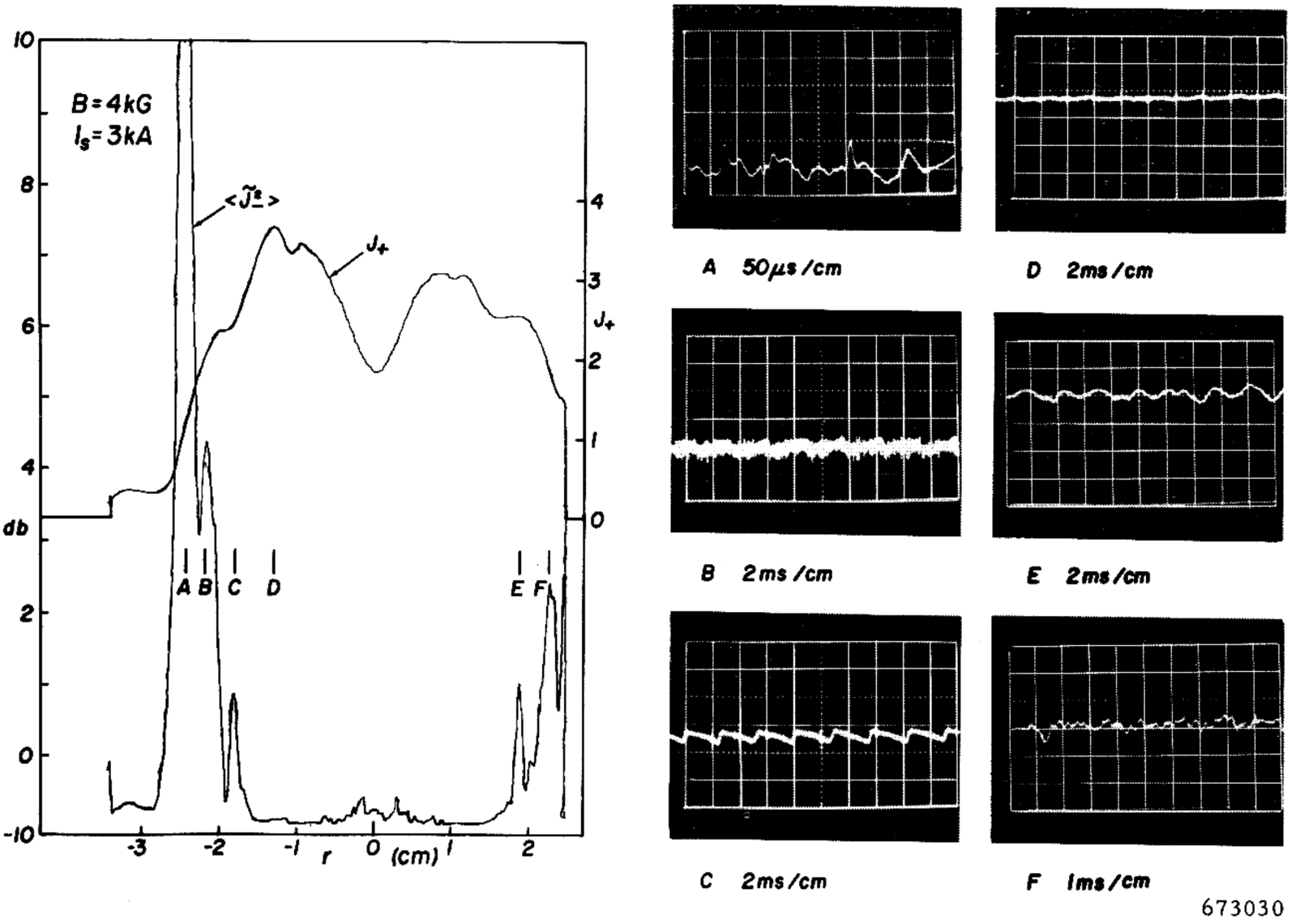

Fig. 13. Density and oscillation profiles at I_s = 3 kA. Other comments of Fig. 11 apply.